J. Electroanal. Chem., 160 (1984) 321–333
Elsevier Sequoia S.A., Lausanne – Printed in The Netherlands

SURFACE-ENHANCED RAMAN SPECTROSCOPY OF ELECTROCHEMICALLY CHARACTERIZED INTERFACES

RELATIONS BETWEEN RAMAN SCATTERING INTENSITY AND SURFACE COVERAGE FOR SIMPLE ANIONIC ADSORBATES

MICHEAL J. WEAVER * and JOSEPH T. HUPP

Department of Chemistry, Purdue University, West Lafayette, IN 47907 (U.S.A.)

FELIX BARZ **, JOSEPH G. GORDON II and MICHAEL R. PHILPOTT

IBM Research Laboratory, San Jose, CA 95193 (U.S.A.)

(Received 29th March 1983)

ABSTRACT

Surface-enhanced raman scattering (SERS) obtained as a function of electrode potential for chloride, bromide, iodide, thiocyanate, azide, and cyanide adsorbed at roughened silver electrodes is compared with corresponding surface concentration-potential data extracted from differential capacitance measurements in order to examine the relation between SERS and surface coverage for these structurally simple adsorbates. After generating SERS by means of an oxidation–reduction cycle, it was found that altering the potential to a more negative value, where the adsorbate coverage fell below a monolayer, corresponded closely in most cases to the onset of a potential-dependent decay in the SERS intensity. Monitoring the potential dependence of the Raman intensity with an optical multichannel analyzer as well as with a conventional scanning spectrometer allowed a rapid "reversible" component of the potential dependence to be separated from an additional "irreversible" signal decay associated with the loss of Raman-active sites. Examination of potential-dependent SERS sufficiently rapidly so that reversible conditions prevail has the crucial advantage of holding constant the concentration of Raman-active sites. For adsorbed chloride and bromide, an approximate correlation was found between the fractional coverage and the variation in the corresponding reversible Raman intensity brought about by altering the electrode potential. The present results suggest that the adsorption energetics of the Raman-active surface sites do not differ substantially from those for the sites occupied by the majority of the adsorbate.

INTRODUCTION

The large number of experimental investigations that have followed the initial discovery of surface-enhanced Raman scattering (SERS) [1] have demonstrated that

* IBM Visiting Scientist, 1981–1982.

** IBM World Trade Postdoctoral Fellow 1981–1982; permanent address: Institut für Physikalische Chemie, Universität Bonn, Wegelerstrasse 12, 53 Bonn, F.R.G.

0022-0728/84/$03.00

a variety of ions and molecules at several metal surfaces can yield easily detectable SERS spectra [2]. The SERS technique is of particular importance to the study of metal-electrolyte interfaces, since in situ molecular spectroscopic probes have previously been unavailable for electrochemical systems. It has become customary to draw inferences concerning the degree of specific adsorption of a given species from the presence (or absence) of the appropriate SERS signals. However, surprisingly few SERS measurements have been accompanied by, or related to, quantitative electrochemical characterization of the surface composition. While SERS has the important and intriguing virtue of molecular specificity for the detection of electrochemical adsorbates, the relation between the Raman intensities and the corresponding surface concentrations of a particular component has remained largely unexplored.

It is clearly important for this purpose to examine the dependence of the SERS intensities for structurally simple adsorbates upon the surface adsorbate concentration as determined by independent means. Such studies, at least of a quantitative nature, are conspicuous by their absence. However, the required surface concentrations for ionic adsorbates can be determined accurately from measurements of the differential double-layer capacitance C_d as a function of the electrode potential E and the bulk adsorbate concentration in mixed electrolytes at a constant total ionic strength by using the so-called "Hurwitz–Parsons" analysis [3,4]. We have recently utilized this technique to obtain surface concentrations for a number of halide and pseudohalide anions at smooth and also electrochemically roughened silver electrodes [5,6]. The latter conditions were chosen so to match those commonly employed to obtain SERS spectra. Only moderate ($\lesssim 2$ fold) increases in the microscopic surface area are brought about by surface roughening, and only mild variations ($\lesssim 30\%$) occur in the adsorbate surface concentration after correction of the changes in surface area [6]. In contrast, the corresponding SERS intensities are extremely sensitive to the surface morphology. The Raman signals commonly decay irreversibly upon altering the potential to more negative values [7], even though the surface concentration–potential data exhibit no detectable hysteresis under these conditions [6]. These results indicate that the SERS intensity is dependent on the effective concentration of "SERS-active sites" as well as the adsorbate concentration, the former being much more sensitive to the surface history [8].

In this article, surface concentration data for chloride, bromide, iodide, thiocyanate, azide, and cyanide are compared with SERS intensities as a function of electrode potential determined under the same, or similar, experimental conditions. The halide adsorbates are of fundamental importance in view of their extreme structural simplicity. The pseudohalide adsorbates exhibit internal vibrational modes in addition to the ligand–surface stretching mode, the intensity of which may be influenced additionally by orientation and surface interaction effects. The potential-dependent SERS data were obtained sufficiently rapidly, using an optical multichannel analyzer (OMA) system as well as a conventional scanning spectrometer, that the irreversible decay of the Raman signal comprised only a negligible part of the observed potential dependence. The results therefore enable the dependences of the

SERS intensity upon the average adsorbate concentration to be examined quantitatively for this archetypally simple class of electrochemical adsorbates.

EXPERIMENTAL

Time-resolved Raman spectra in the region 100–2200 cm^{-1} were obtained with an OMA system consisting of a PAR Model 1420 detector, Model 1418 Controller, and Model 1215 console, coupled to a SPEX Model 1877 spectrograph. Under favorable conditions, good-quality spectra could be obtained repetitively in as little as 0.1 s. Raman spectra in the region 100–2300 cm^{-1} were also recorded using a scanning spectrometer system based on a SPEX Model 14018 double monochromator. A Coherent Radiation CR-3000K Krypton laser operated at 530.9 or 647.1 nm was used for Raman excitation. Further details are given in ref. 9.

Differential capacitance measurements were made using a phase sensitive detection method as outlined in ref. 6. The working electrode for both the Raman and capacitance measurements was a polycrystalline silver rod (assay > 99.999%). For the latter measurements the electrode was sheathed in Teflon in order to expose a well-defined area [6]. The laser beam was focused on an approximately 1×5 mm line on the surface, the total incident power being typically 100–200 mW. The electrode was mechanically polished with 1.0 and then 0.3 μm alumina, rinsed rapidly with water, and then roughened by means of an oxidation-reduction cycle (ORC) using a double potential step in the electrolyte of interest, generally passing 20–30 mC cm^{-2} charge during the anodic pulse. All electrolytes were prepared using doubly distilled water and recrystallized salts, and deoxygenated by bubbling with prepurified nitrogen. Electrode potentials are quoted with respect to the saturated calomel electrode (SCE). All measurements were made at room temperature, 23 ± 0.5°C.

RESULTS

Chloride electrolytes

Adsorption data at electrochemically roughened silver electrodes for halide or pseudohalide anion, X^-, were determined from C_d–E measurements for a series of mixed electrolytes of general composition $(0.5 - x)$ M $NaClO_4 + x$ M NaX, with x in the range 0–0.1 M. Sodium perchlorate was chosen as the base electrolyte because of the weak adsorption of perchlorate and the relative frequency-independence of the measured capacitance at roughened as well as smooth electropolished silver in this medium [6]. For chloride, SERS were examined with $x = 10^{-3}$, 10^{-2}, and 0.1 M. Oxidation–reduction cycles were performed between -100 and 300 mV, generally in the presence of laser illumination to further enhance the intensity of the resulting SER signals [10]. A Raman signal with a peak at approximately 240 cm^{-1} appeared during the cathodic portion of the ORC [11] with an intensity that was almost independent of the bulk chloride concentration, although it slowly decayed with time

(approximate "half-time" $t_{1/2} \sim 1$ h at 0 mV). Similar results have been obtained previously [7,12–14]; the 240 cm^{-1} band is consistent with a surface–chloride stretching mode [15]. The temporal development of the SERS signals during potential sweep and step ORCs observed for chloride and other adsorbates using the OMA system will be discussed in detail elsewhere [11]. (Although weaker signals were often obtained for anionic adsorbates in the absence of laser irradiation during the ORC, the potential and time dependence of the relative intensities were essentially independent of the extent of laser irradiation both during and following the ORC. The capacitance data were generally obtained in the absence of laser illumination, although essentially identical results were obtained for chloride electrolytes in the presence of such irradiation.)

Alteration of the electrode potential to values negative of 0 mV vs. SCE where the interface approaches ideal polarizability (i.e. where only nonfaradaic currents flow) produced two major effects that were most easily distinguished by rapidly recording successive spectra in the 150–300 cm^{-1} region using the OMA. Stepping the potential to successively more negative values from ca. 0 mV yielded immediate (< 1 s) decreases in the intensity of the 240 cm^{-1} band that diminished to undetectable levels in comparison with the continuum background at about −1000 mV. Providing that the potential was returned to the original (least negative) value sufficiently rapidly (vide infra), the Raman signal recovered almost to its original level, i.e. the intensity-potential dependence was essentially reversible. However, holding the potential at a given more negative value resulted in a gradual decay in the signal intensity. This latter potential dependence is associated with an irreversible decay process since the Raman intensity does not recover upon returning the potential to the original less negative value [7]. The decay process was found to become progressively more rapid with increasing negative electrode potential; typically $t_{1/2}$ decreased from ca. 60 min at potentials positive of −100 mV to 15 min at −350 mV and 8 min at −550 mV. A typical first-order rate plot of $\log(I_p^i/I_p^t)$ vs. time, where I_p^i is the initial background-corrected peak intensity following a potential step from 0 mV to −350 mV, and I_p^t is the corresponding intensity at time t, is shown in Fig. 1. The electrolyte was 0.4 *M* $NaClO_4$ + 0.1 *M* NaCl. A noticeable deviation from first-order kinetics is seen (Fig. 1) for $I_p^t/I_p^i \lesssim 0.5$, similar to that seen previously for thiocyanate at silver [9].

This irreversible signal decay is difficult to avoid at the more negative potentials using a scanning spectrometer since at least 5–10 min are typically required in order to acquire a single spectrum. On the other hand, spectra could easily be recorded sufficiently rapidly with the OMA to ensure reversible behavior. A plot of the Raman peak intensity with respect to that at 0 mV, $I_p^i/I_p^i(0\text{ mV})$, against electrode potential E in 0.4 *M* $NaClO_4$ + 0.1 *M* NaCl under reversible conditions is shown as a dashed line in Fig. 2. This plot is an average of several runs using both the OMA and the scanning spectrometer systems. (Similar results were obtained if the total integrated intensity of the Raman band was plotted instead of the peak intensity.) The solid line also shown in Fig. 2 is a plot of the corresponding fractional surface coverage of chloride ions at roughened silver, θ, against E for the same electrolyte.

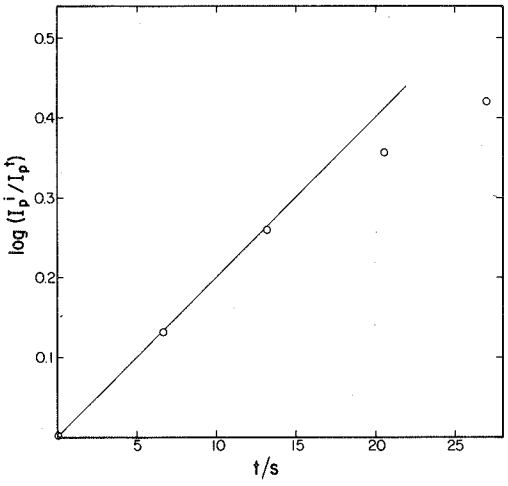

Fig. 1. First-order rate plot of $\log(I_p^i/I_p^t)$ vs. time for decay of Raman peak intensity for surface–Cl^- stretching mode at -350 mV, where I_p^i is initial background-corrected peak intensity and I_p^t is corresponding intensity at time t. Electrolyte was 0.4 M $NaClO_4 + 0.1$ M NaCl. Straight line is slope of curve at $t = 0$.

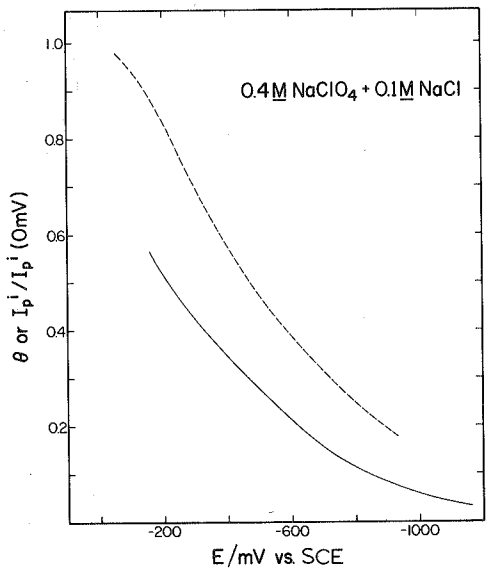

Fig. 2. Fractional coverage, θ, of chloride anions (solid curve) and reversible Raman peak intensity I_p^i/I_p^i (0 mV), for Ag–Cl^- stretching mode relative to that at 0 mV, (dashed curve), both plotted against electrode potential, E, using the same scale. Electrolyte was 0.4 M $NaClO_4 + 0.1$ M NaCl.

This line is plotted using the same axes as the Raman data. The values of θ were obtained from the corresponding chloride surface concentrations, Γ'_{Cl}, in ref. 6 together with the saturation value of Γ'_{Cl}, $\Gamma'_{sat} = 1.6 \times 10^{-9}$ mol cm^{-2} [6], using $\theta = \Gamma'/\Gamma'_{sat}$. The values of θ are reproducible to ca. $\pm$5–10%, and the values of $I^i_p/I^i_p(0\text{ mV})$ to ca. $\pm$10–15%.

It is seen from Fig. 1 that the potential dependence of the Raman intensity for chloride-surface stretching approximately follows that of the chloride surface concentration. Admittedly the values of $I^i_p/I^i_p(0\text{ mV})$ are somewhat larger than θ at all potentials. This apparent discrepancy probably arises, at least in part, from the likelihood that the chloride surface coverage is smaller than unity even at 0 mV. Electrolytes containing from 10^{-3} to 0.1 *M* chloride yielded plots of $I^i_p/I^i_p(0\text{ mV})$ vs. *E* that were almost coincident within the experimental uncertainty. Although at first sight this result is surprising, scrutiny of the corresponding adsorption data for chloride and other anions [6] reveals that Γ increases only slightly (ca 10%) at a given potential for even a tenfold increase in bulk concentration, c_b. This insensitivity of Γ' (and hence θ) to variations in c_b arises from the strong repulsive interactions between the adsorbed anions [6].

The peak frequency of the surface–chloride stretching ν_{Cl}, was also found to be significantly dependent on the electrode potential. Although the exact value of ν_{Cl} varied slightly (2–3 cm^{-1}) with experimental conditions at a given electrode potential, it typically decreased linearly with increasing negative potential, with $d\nu_{Cl}/dE \sim 15$–20 cm^{-1} V^{-1} (cf. ref. 7). The Raman bands were relatively broad, the full width at half peak maximum (FWHM) being 40–45 cm^{-1}.

Bromide

Bromide ions are sufficiently more strongly adsorbed than chloride at silver to yield essentially a monolayer at potentials positive of -300 mV for bulk bromide concentrations in the range ca 5–100 m*M*, as deduced from the constant and potential-independent values of C_d obtained under these conditions [6]. Similarly to chloride, the bromide surface concentration Γ'_{Br} decreases with increasing negative potential, the coverage falling below 10% beyond ca -1100 mV [6]. Bromide therefore provides an especially tractable adsorbate with which to study the dependence of the Raman scattering intensity upon adsorbate coverage.

Oxidation–reduction cycles from -200 to $+100$ mV in perchlorate-based electrolytes containing bromide yielded silver surfaces exhibiting a Raman band at about 160 cm^{-1}, consistent with surface–bromide stretching [7,13–15]. Satisfactorily strong Raman signals were obtained by irradiating with red light (647.1 nm) during the ORC [10]. The band intensity was essentially independent of potential from the positive polarization limit, ca -150 mV, to about -300 mV, consistent with the presence of a bromide monolayer (i.e. $\theta = 1$) within this region. The signal slowly decayed with time under these conditions, although it was stable on the time scale of most experiments (ca. 30–60 min). Similarly to chloride, altering the potential to values where the anion coverage is below unity yielded progressive decreases in I^i_p

and also accelerated the rate of irreversible decay of the Raman signal. Although accurate measurement of the peak frequency, ν_{Br}, for the Ag–Br^- stretching mode was hampered by its proximity to the Raleigh "tail", as for chloride it decreased significantly with increasing negative potential, with $d\nu_{Br}/dE \sim 10$–15 cm^{-1} V^{-1}. Again, by recording the Raman spectra at each potential within a time scale short compared with that over which the irreversible decay occurs (typically a few minutes) the potential dependence of the reversible component of I_p, I_p^i, could be obtained. A plot of $I^i/I_p^i(sat)$ against E, where $I_p^i(sat)$ is the Raman intensity for a bromide monolayer at -200 mV, is shown as a dashed line in Fig. 3. These data were gathered using the electrolyte composition 0.45 M $NaClO_4$ + 50 mM NaBr; virtually indistinguishable results were obtained, however, using 5 to 100 mM bromide. (Satisfactory data could not be obtained for $I_p^i/I_p^i(sat) < 0.2$, where the Raman signal was insufficiently stable and also buried in the "tail" of Raleigh-scattered light.) The corresponding plot of θ against E, plotted on the same axes as the dashed curve, is shown as a solid line in Fig. 3. This was obtained from data given in ref. 6 assuming that a bromide monolayer corresponds to $\Gamma'_{sat} = 1.35 \times 10^{-9}$ mol cm^{-2} [6].

A reasonable correlation between the potential dependence of the reversible Raman intensity and the bromide coverage is seen in Fig. 3, although the values of $I_p^i/I_p^i(sat)$ are noticeably greater than θ at all potentials where $\theta < 1$.

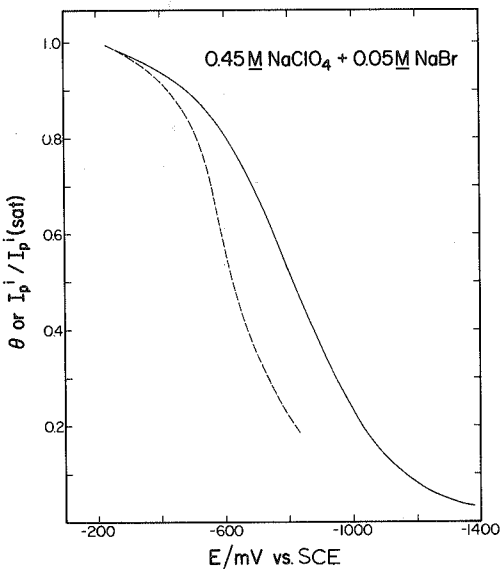

Fig. 3. Fractional coverage, θ, of bromide anions (solid curve) and reversible Raman peak intensity, $I_p^i/I_p^i(sat)$, for Ag–Br^- stretching mode relative to that for bromide monolayer (dashed curve), both plotted against electrode potential, E, using the same scale. Electrolyte was 0.45 M $NaClO_4$ + 0.05 M NaBr.

Iodide

Roughening silver surfaces in contact with perchlorate-based electrolytes containing iodide anions (1–100 mM) by using an ORC between −350 and 0 mV yielded a Raman peak at 120 cm^{-1} due to a surface–I^- stretching mode [7,13–15]. Suitably strong signals were obtained by illuminating the surface with 647.1 nm rather than 530.9 nm radiation during the ORC (cf. ref. 7), although the peak is at sufficiently small Raman frequencies to be distorted somewhat by the Raleigh "tail" of stray light within the spectrometer system. In contrast to chloride and bromide, the background-corrected intensity of the surface–iodide mode only decreases slightly (ca 10%) between −300 and −800 mV, although the level of the continuum background increases by almost twofold over this range. The Raman intensity decreases sharply at potentials more negative than about −900 mV, falling to almost imperceptable levels by −1200 mV. Similar results were obtained by Wetzel et al. [7] (SERS data for adsorbed iodide were not obtained using the OMA because of excessive interference from stray Raleigh scattered light).

The usual "Hurwitz–Parsons" analysis of the C_d–E data could not be used to obtain iodide surface concentrations, Γ_I'. This is because C_d increases sharply with increasing bulk iodide concentration even at the most negative potentials (−1400 mV); thus no potential is available at which Γ_I' is sufficiently small to allow the required back integration of the C_d–E curves to be undertaken [6]. However, as for bromide, the point where the iodide coverage falls below a monolayer for a given electrolyte composition can be deduced simply from the shape of the C_d–E curves. Thus within the potential region −300 to −800 mV the capacitance is almost

TABLE 1

Comparison between threshold potential, E_{th}, of SERS intensity–potential dependence for anion adsorbates and potential for onset of anion desorption, E_d, extracted from capacitance data

Anion adsorbate	Electrolyte	E_{th}/ mV vs. SCE [a]	E_d/ mV vs. SCE [c]
Chloride	(0.01–0.1) M NaCl + 0.5 M $NaClO_4$	$\gtrsim -100$	~ 0
Bromide	(0.01–0.05) M NaBr + 0.5 M $NaClO_4$	−300 to −400	−400 to −500
Iodide	0.01 M NaI + 0.5 M $NaClO_4$	−900	−800 to −900
Thiocyanate	0.01 M NaNCS + 0.5 M $NaClO_4$	−200	ca. −800
Azide	0.5 M NaN_3	$\gtrsim 50$ [b]	~100
Cyanide	0.01 M KCN + 0.05 M Na_2SO_4	−1050	ca. −1000 [d]

[a] From present work except where indicated.
[b] From data in ref. 19.
[c] Estimated as noted in text, using capacitance–potential data in ref. 6 except where indicated.
[d] From data in ref. 16.

independent of iodide concentration and potential, indicating that a monolayer of iodide is present [6]. Beyond -800 mV C_d rises sharply, signalling that the iodide coverage falls below a monolayer. We shall term this point at which anion desorption commences the "desorption potential", E_d. Similarly to bromide and chloride, the "threshold potential", E_{th}, marking the onset of the reversible potential dependence of the iodide SERS intensity, ca -900 mV, is close to the corresponding value of E_d. A summary of values of E_d and E_{th} for each adsorbate is given in Table 1.

Pseudohalide anions

We have recently compared in detail the potential dependence of SERS for adsorbed thiocyanate at silver with the corresponding surface concentration data obtained from C_d–E curves [9]. In contrast to halide adsorbates, the reversible component of bands due to surface–sulfur and C–N stretching modes decrease noticeably (2–3 fold) with increasing negative potential in the region ca -100 to -700 mV, even though the thiocyanate coverage remains close to a monolayer throughout [9]. The C_d–E curves for adsorbed thiocyanate also differ from those for adsorbed halides in that the former show a marked "structure", with one, and under some conditions two, major peaks within the potential region (-100 to -800 mV) over which the SERS signals undergo profound changes [6].

The comparison between SERS and C_d–E data for adsorbed thiocyanate and cyanide is instructive in this regard. Capacitance data are available at smooth silver for 1 M Na_2SO_4 with various concentrations of NaCN [16]. Similarly to thiocyanate, cyanide is sufficiently strongly adsorbed to yield substantial increases in C_d at extremely negative potentials (-1000 to -1500 mV) [16]. As for the halides [6], the presence of a plateau in the C_d–E curves at ca -1000 mV vs. SCE for the highest CN^- concentration (3 mM) indicates the onset of saturation coverage at this point [16]. (Admittedly, the corresponding calculated surface concentrations, ca 5×10^{-10} mol cm^{-2}, are somewhat smaller than that expected for a close-packed cyanide layer [16].) SERS data for the C–N stretching mode (ca. 2110 cm^{-1}) of adsorbed cyanide were measured using a similar electrolyte, 0.05 M Na_2SO_4 + 0.01 M NaCN. Similarly to bromide and iodide but in contrast to thiocyanate, the intensity of the C–N stretching mode is almost independent of potential within the potential region, -700 to -1000 mV, where the adsorbed cyanide is present at close to monolayer levels. The sharp drop in Raman intensity only commences at a potential, E_{th} ~ 1050 mV, close to the corresponding "desorption potential", E_d ~ -1000 mV [14]. Essentially the same results were obtained by Wetzel et al. [17] for the Ag–CN^- (220 cm^{-1}) as well as the C–N stretching mode. The peak frequency, ν_{CN}, of the C–N stretching mode was also found to be potential dependent, with $d\nu_{CN}/dE \sim 25$ cm^{-1} V^{-1} (cf. refs. 17, 18).

Azide also provides an interesting comparison with thiocyanate in view of their structural similarity. A recent SERS study of azide adsorbed at silver showed that stable Raman signals, including those corresponding to the Ag–N_3^- and N–N stretching modes, were only obtained at potentials, ca. 50 mV vs. SCE, close to the

onset of silver oxidation [19]. The spectra disappeared, at least on the time scale required for the scanning spectrometer measurements, at more negative potentials [19]. This result is again consistent with the capacitance data in that saturation coverages of azide are only approached at potentials, ca. 100 mV, near the positive polarization limit in solutions containing $\gtrsim 0.01$ M azide [6]. Therefore, the approximate correspondence between E_{th} and E_d also appears to hold for azide (Table 1).

DISCUSSION

The consistently close correspondence between the threshold potential for the SERS intensity-potential dependence, E_{th}, and for the onset of anion desorption, E_d, (Table 1) indicates that anion coverages close to a monolayer are normally required in order to obtain SERS signals for these adsorbates that have long-term stability. This can simply be understood in terms of a model whereby Raman scattering occurs from specific surface sites associated with particular silver structures which are metastable with respect to incorporation into the surface metal lattice. Although it has been suggested that these sites are individual adatoms [7,8,17], they are more likely to be metal clusters [9,10,20]. Under conditions where the anion coverage approaches a monolayer, anions will not only bind to these sites yielding SERS but will also occupy almost all the remaining metal lattice sites. Although not contributing directly to the observed Raman signal, the latter adsorbate can stabilize the Raman-active clusters by preventing their dissipation into the metal lattice [9]. Altering the potential to sufficiently negative values where a fraction of this adsorbate is immediately desorbed provides vacant lattice positions into which the least stable clusters can gradually dissociate, thereby accounting for the observed irreversible decay of the Raman intensity under these conditions (Fig. 1).

This model also accounts for the observed dependence of the decay kinetics upon the electrode potential; indeed the irreversible decay rates for chloride appear to be related to the availability of "open" lattice sites as estimated by $(1 - \theta)$. The observed deviation of the kinetics from a first-order rate law (Fig. 1) suggests that there is a progressive increase in the activation energy as the decay process proceeds [9]. This is consistent with a distribution in the structure and hence stability of the Raman-active clusters. Such a distribution may in part be responsible for the broad Raman bands typically seen for the present anionic adsorbates; surface sites having differing geometries and adsorbate binding energies are expected to yield distinct SERS vibrational frequencies. The breadth of the Raman bands are also attributable to electrostatic interactions between nearby adsorbate ions [21].

Nevertheless, the correlations between the corresponding reversible variations in the Raman intensity and the adsorbate coverage for chloride and bromide (Figs. 2 and 3) indicate that the adsorption energetics at the Raman-active sites do not differ substantially from those for the entire surface as determined from the capacitance data. That such correlations are only very approximate is to be expected on several grounds. Firstly, this may be due in part to systematic errors in the estimation of θ

and $I_p^i/I_p^i(sat)$. Secondly, the Raman scattering efficiency itself may well depend on the surface composition and/or the electrode potential, so that I_p^i will not be linearly related to the degree of adsorbate occupancy of the total available Raman-active sites. Thirdly, the Raman-active sites probably constitute only a small fraction of the overall surface. This last possibility is evidenced by the entirely reversible nature of the C_d–E curves under the same conditions that the potential dependence of I_p^i exhibits almost total irreversibility [6]. Therefore the structures, and hence adsorption properties, of the Raman-active sites may differ somewhat from the majority sites which dominate the measured thermodynamic properties. Indeed, the thermodynamics of chloride adsorption as well as the potential of zero charge at the (*111*) surface plane of silver differ significantly from those at the (*100*) and (*110*) low index planes [22]. The morphology of the C_d–E curves at the electrochemically roughened as well as electropolished silver surfaces are consistent with the presence of a conglomeration of these crystal planes [6]. Nevertheless, at a given electrode potential the chloride surface concentrations at the three low index planes are only marginally different (ca. 10–20%) for the intermediate surface coverages ($\gtrsim 0.2$) of interest here [22], thereby suggesting that other metal lattice configurations (such as metal clusters) may also exhibit comparable occupancies by chloride anions.

It has frequently been suggested (e.g. refs. 23–25) that SERS arises from "surface complexes" where one or more of the Raman-active species are bound to a single metal atom, presumably displaced from its normal position in the metal lattice. Such structures have been proposed in particular for species such as cyanide that are known to multiply coordinate to Ag(I). However, the distinction between adsorption and "surface complex" formation is not clearcut, especially if the Raman-active species are associated with metal clusters rather than isolated adatoms. In any case, the approximate relationship between the SERS intensity and the average adsorbate coverage for bromide and chloride provides an argument against the need to invoke distinct "surface complexes" for these systems.

Of the six anionic adsorbates considered here, thiocyanate, cyanide, bromide, and iodide are sufficiently strongly adsorbed to enable SERS to be observed over a significant potential range (say $\gtrsim 200$ mV) between the onset of monolayer formation (i.e. E_d) and silver oxidation. Thiocyanate exhibits somewhat different behavior to cyanide, bromide, and iodide in that the SERS signals for the former decrease sharply in intensity as the potential is made more negative even in the region positive of E_d [9]. The most likely explanation is that the thiocyanate layer undergoes a structural rearrangement as the potential is altered. Although thiocyanate almost certainly binds to the surface preferentially via the sulfur atom [6,9], coordination additionally via the nitrogen atom is feasible, which could result in a relative flat orientation. As the potential is made more positive, the enhanced electric field, together with the greater driving force for high packing densities, should increasingly favor a more vertical orientation [6]. The latter orientation would provide more efficient Raman scattering, especially for the internal modes (C–N, C–S stretching), since the component of polarization normal to the surface would thereby be enhanced [26]. Such a reorientation change therefore provides a simple explanation

of the increased SERS intensities as the potential is made more positive in the -100 to -800 mV region. It also accounts for the enhanced stability of the Raman signals under these conditions since dissociation of the SERS-active metal clusters should be retarded especially by close-packed, vertically bound, thiocyanate. The broad capacitance peaks seen for adsorbed thiocyanate within this potential region provide further evidence for such structural changes [6].

The significant decreases in the peak frequencies, ν_x, of both surface–anion and internal adsorbate vibrational modes with increasing negative potential have commonly been asserted to be due to a weakening of the bonds caused by shifts in bond polarization as the electronic surface charge on the metal becomes decreasingly positive and eventually negative [7,13,14,17,18,27]. However, this argument becomes less persuasive for most adsorbates upon consideration of the electrosorption valencies for such simple anionic adsorbates at silver, which suggest that the surface bonds are predominantly ionic [5]. A difficulty with interpreting potential dependencies of ν_x purely in terms of adsorbate–surface interactions is that for most of these systems the surface coverage is also changing with potential over most of the accessible potential region. This provokes the suggestion that the potential dependence of ν_x may be due in part to the concomitant variations in surface composition. Indeed, recent theoretical calculations indicate that the effective value of ν_x for halide adsorbates at silver decreases noticeably as the coverage diminishes as a result of changes in adsorbate–adsorbate interactions [21]. (These calculations also predict that the Raman bands should exhibit definite coverage-dependent structural features [21]. Such features have been observed for halide SERS in colloidal [28], as well as electrochemical, systems [7]. However, single Raman peaks without noticeable inflections or marked asymmetry were typically obtained in the present work). As noted above, the characteristically broad Raman bands for anionic adsorbates (FWHM ~ 30–50 cm^{-1}) suggest that a range of surface structures contribute to SERS. The preferential desorption of anions associated with higher vibrational frequencies as the potential is made more negative can therefore also account for the observed decreases in ν_x since ν_x is actually an ensemble average. The experimental separation of these various coverage- and potential-dependent factors will require careful measurements of the potential dependence of ν_x for adsorbates, such as iodide, that can be studied over wide potential ranges at a constant surface coverage.

Nevertheless, the approximate correlations seen here between the SERS intensity and the surface concentration of halide adsorbates is most encouraging. The above considerations demonstrate the value not only of obtaining SERS at surfaces for which separate information on the composition and structure can be obtained, but also of selecting experimental conditions such that the concentration of Raman-active surface sites can be held essentially constant throughout the spectroscopic measurements. This highlights the desirability of obtaining Raman spectra rapidly by using a spectrograph-optical multichannel analyzer detector. Such strategies enable the relation between SERS and the electrochemical surface composition and structure to be assessed quantitatively, thereby paving the way for application of the SERS technique to a variety of electrochemical problems.

ACKNOWLEDGEMENTS

The research program of M.J.W. is supported in part by the Office of Naval Research and the Air Force Office of Scientific Research.

REFERENCES

1 (a) M. Fleischmann, P.J. Hendra and A.J. McQuillan, Chem. Phys. Lett., 26 (1974) 163; (b) D.L. Jeanmaire and R.P. Van Duyne, J. Electroanal. Chem., 84 (1977) 1; (c) M.G. Albrecht and J.A. Creighton, J. Am. Chem. Soc., 99 (1977) 5215.
2 For reviews, see (a) R.P. Van Duyne in C.B. Moore (Ed.), Chemical and Biochemical Applications of Lasers, Academic Press, New York, Vol. 4, 1979, Ch. 5; (b) T.E. Furtak and J. Reyes, Surf. Sci., 93 (1980) 382; (c) R.L. Birke, J.R. Lombardi and L.A. Sanchez, Am. Chem. Soc. Adv. Chem. Ser., 201 (1982) 69.
3 (a) H.D. Hurwitz, J. Electroanal. Chem., 10 (1965) 35; (b) E. Dutkiewicz and R. Parsons, ibid., 11 (1966) 100.
4 M.J. Weaver and F.C. Anson, J. Electroanal. Chem., 65 (1975) 737.
5 D. Larkin, K.L. Guyer, J.T. Hupp and M.J. Weaver, J. Electroanal. Chem., 138 (1982) 401.
6 J.T. Hupp, D. Larkin and M.J. Weaver, Surf. Sci., 125 (1983) 429.
7 For example, see H. Wetzel, H. Gerischer and B. Pettinger, Chem. Phys. Lett., 78 (1981) 392.
8 A. Otto in M. Cardona and G. Güntherodt (Eds.), Light Scattering in Solids, Vol 4, Springer, Berlin, 1983; A. Otto, Appl. Surf. Sci., 6 (1980) 309.
9 M.J. Weaver, F. Barz, J.G. Gordon II and M.R. Philpott, Surf. Sci., 125 (1983) 409.
10 F. Barz, J.G. Gordon II, M.R. Philpott and M.J. Weaver, Chem. Phys. Lett., 91 (1982) 291.
11 M.R. Philpott, F. Barz, J.G. Gordon II and M.J. Weaver, J. Electroanal. Chem., 150 (1983) 399; F. Barz, J.G. Gordon II, M.R. Philpott and M.J. Weaver, in preparation.
12 M. Fleischmann, P.J. Hendra, I.R. Hill and M.E. Premble, J. Electroanal. Chem., 117 (1981) 243.
13 B. Pettinger, M.R. Philpott and J.G. Gordon II, J. Phys. Chem., 85 (1981) 2746.
14 J.F. Owen, T.T. Chen, R.K. Chang and B.L. Laube, Surf. Sci., in press.
15 H. Nichols and R.M. Hexter, J. Chem. Phys., 74 (1981) 2059.
16 N.A. Rogozhnikov and R.Y. Bek, Sov. Electrochem., 16 (1980). 67, 564.
17 H. Wetzel, H. Gerischer and B. Pettinger, Chem. Phys. Lett., 80 (1981) 159.
18 R. Kotz and E. Yeager, J. Electroanal. Chem., 123 (1981) 335.
19 R.E. Kunz, J.G. Gordon II, M.R. Philpott and A. Girlando, J. Electroanal. Chem., 112 (1980) 391.
20 W.J. Plieth, J. Phys. Chem., 86 (1981) 3166.
21 H. Nichols and R.M. Hexter, J. Chem. Phys., 76 (1982) 5595.
22 G. Valette, A. Hamelin and R. Parsons, Z. Phys. Chem., N.F. 113 (1978) 71.
23 A. Otto, Surf. Sci., 92 (1980) 145.
24 B. Pettinger and H. Wetzel, Ber. Bunsenges, Phys. Chem., 85 (1981) 473.
25 M. Fleischmann, I.R. Hill and M.E. Premble, J. Electroanal. Chem., 136 (1982) 361.
26 C.S. Allen and R.P. Van Duyne, Chem. Phys. Lett., 63 (1979) 455; G.C. Schatz and R.P. Van Duyne, Surf. Sci., 101 (1980) 425.
27 A.B. Anderson, R. Kotz and E. Yeager, Chem. Phys. Lett., 82 (1981) 130.
28 R.L. Garrell, K.D. Shaw and S. Krimm, J. Chem. Phys., 75 (1981) 4155.